MAPPING THE INNERMOST REGIONS OF AGNS WITH SHORT TIMESCALE FE LINE VARIABILITY

Giovanni Miniutti, Kazushi Iwasawa, and Andrew C. Fabian

Institute of Astronomy, Madingley Road, Cambridge CB3 0HA, UK

ABSTRACT

A relatively narrow emission line feature is seen at 6.1 keV in the X–ray spectrum of the Seyfert galaxy NGC 3516 with *XMM–Newton*. The energy of the feature does not correspond to atomic transitions with large enough probability to occur and is most likely redshifted iron emission (6.4 keV). We study its short timescale variability which reveals both flux and energy modulations on a characteristic timescale of 25 ks. The variations agree with an orbiting spot model in which an Fe line is emitted from a localized spot on the accretion disc, illuminated by a corotating flare above it. The spot is located at about $10\,r_g$ from the black hole and almost four cycles of orbital modulation are seen. By combining the spot location with the orbital timescale we can estimate the black hole mass in NGC 3516 which turns out to be in excellent agreement with reverberation mapping results, supporting our interpretation in terms of relativistic effects close to the black hole. *XMM–Newton* proves here able to map with high accuracy the inner accretion flow in AGNs down to the relativistic region of the curved spacetime in the immediate vicinity of the accreting black hole.

Key words: X–rays: galaxies; galaxies: active; galaxies: individual: NGC 3516; relativity.

1. INTRODUCTION: FE EMISSION FROM ACCRETION DISCS

A substantial fraction of the accretion energy in luminous Active Galactic Nuclei (AGNs) is thought to be dissipated in the inner regions of the accretion flow around the central black hole. Most bright AGNs are believed to have accretion efficiencies of at least 10 per cent which requires the flow to be radiatively efficient down to only few gravitational radii ($r_g = GM/c^2$ where M is the black hole mass) from the black hole, where both special and general relativity are likely to play a fundamental role. X–rays provide a unique vue of the innermost regions of accreting black holes and time–resolved spectroscopy has the great potential of mapping the accretion flow and even the spacetime geometry in the immediate vicinity of black holes.

One of the most powerful tool we have to investigate the nature of the innermost accretion flow in AGNs is provided by the X–ray reflection spectrum from the accretion disc. The main feature of the reflection spectrum is the iron (Fe) K fluorescent line with rest–frame energy between 6.4 keV and 6.96 keV depending on the ionization state of the reflector. If the Fe line originate from the accretion disc, high velocities and strong gravity effects produce distortions on the line profile that can be used to infer the main properties of the accretion flow and the geometry of the spacetime close to the black hole. In fact, each ring on the accretion disc produces a symmetric double–horned line profile corresponding to emission from the approaching and receding sides of the disc with respect to the observer. As one approaches the central black hole, orbital velocities become relativistic and relativistic beaming enhances the blue peak of the line with respect to the red one. Finally, transverse Doppler and gravitational redshift produce a shift to lower energies of the emission from each ring on the disc. The overall line profile from the accretion disc is obtained by summing the contributions from all radii. The resulting line profile is asymmetric and broad.

The best example of a broad relativistic line in an AGN is that of MCG–6-30-15 (Tanaka et al 1995; Wilms et al 2001; Fabian et al 2002 and many others). In this case, the red wing of the line extends below 4 keV implying that the accretion disc extends within the innermost stable circular orbit of a non–rotating black hole and thus strongly suggesting that the black hole in MCG–6-30-15 is rapidly spinning, providing evidence for the astrophysical relevance of the Kerr solution of the Einstein's field equations. In Fig. 1 we show another example of a broad relativistic Fe line from a stellar–mass Galactic black hole in outburst, XTE J1650–500. The broad line was discovered by *XMM–Newton* (Miller et al 2004) and we show the result of a *BeppoSAX* observation performed 10 days later during the same 2001 outburst (Miniutti, Fabian & Miller 2004). The detection of a high frequency QPO during the time of the *BeppoSAX* observation (Homan et al 2003) strongly argues in favour of small accretion disc radii. Indeed, the extent of the red wing in the *BeppoSAX*

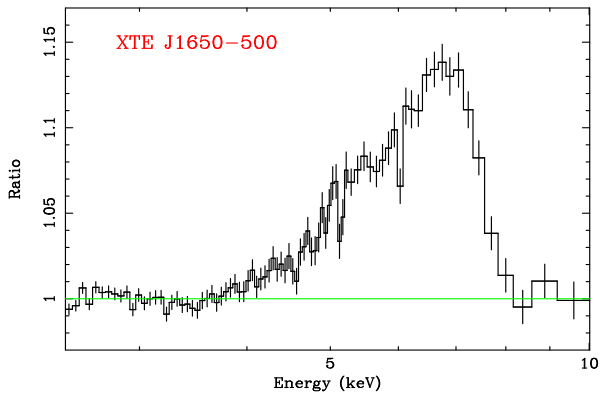

Figure 1. We show the broad Fe line in the Galctic black hole XTE J1650–500. The data were collected by BeppoSAX on 2001 September 21 (Miniutti, Fabian & Miller 2004). See also Miller et al (2004) for the same broad line detected with XMM–Newton 10 days earlier during the same outburst and Rossi et al (2005) for a spectral and variability analysis based on RXTE data.

and *XMM–Newton* data suggest that the accretion disc extends down to about 2 r_g from the black hole, indicating, once again, that the black hole is rapidly spinning.

2. ENERGY–SHIFTED EMISSION LINES

In addition to the major Fe K line at 6.4 keV (often narrow and coming from distant material, sometimes broad and coming from the inner accretion disc), emission features at energies generally lower than 6.4 keV have been observed in the X–ray spectra of several AGNs. An early example was seen with *ASCA* in MCG–6-30-15 (Iwasawa et al 1999) in which the redshifted emission was associated to Fe fluorescence from a localized spot on the disc induced by irradiation from a flare located only few r_g from the black hole. More detections followed in recent years mainly thanks to the improved sensitivity of present X–ray mission such as *Chandra* and *XMM–Newton*. The most remarkable cases reported so far are those of NGC 3516 (Turner et al 2002; Dovčiak et al 2004; Iwasawa, Miniutti & Fabian 2004), NGC 7314 (Yaqoob et al 2003), ESO 198–G24 (Guainazzi 2003; Bianchi et al 2004), Mrk 766 (Turner, Kraemer & Reeves 2004), ESO 113–G10 (Porquet et al 2004), and AX J0447–0627 (della Ceca et al 2005). In all the above cases, the energy at which these emission features are detected does not correspond to any atomic transition with large enough probability to occur to be detected in the X–ray spectra of AGNs. The most natural and likely explanation is that these features are Fe K emission lines which have been redshifted to the observed energies by a kinematical and/or gravitational mechanism.

In Fig. 2 we show two examples of redshifted detected features. In the left panel we show the hard spectrum and data to model ratio from the first *XMM–Newton* observation of ESO 198–G24 (Guainazzi 2003). Besides emission around 6.4 keV, an emission line is detected at 5.7 keV. In a subsequent observation, the line was found at 5.9 keV but only in the second half of the observation suggesting a transient nature and short–timescale variability (Bianchi et al 2004). In the right panel of the same figure, we show the spectrum and data to model ratio (a simple power law is assumed) for the *XMM–Newton* observation of ESO 113–G10 (Porquet et al 2004). An emission feature is clearly seen at 5.4 keV in the source rest–frame and a detailed statistical analysis shows it is significantly detected (about 99 per cent confidence level according to Montecarlo simulations, see Porquet et al 2004).

2.1. Short–timescale variability: orbiting spots?

A tentative, exciting, but not unique explanation for the observed redshifted emission features is that we are looking at Fe emission originating in a localized region on the accretion disc (hereafter "spot"). In this picture, the spot is produced by irradiation from a localized magnetic flare above the disc which produces the Fe line by fluorescence in the surface layers of the disc. The redshift of the observed lines is due to the location and velocity of the flare/spot system, combined with the disc inclination with respect to the observer. The simplest assumption is that the flare, linked by magnetic fields to the disc, participates to the disc Keplerian motion. As shown in Dovčiak et al (2004) and Pecháček et al (2005), such a model could indeed explain most of the observed features. The idea is that if the integration time is longer than the spot orbital period, emission from a narrow ring will be seen. The Fe line emitted from such a ring is generally narrow and redshifted, as seen in most data. If the data are interpreted in this framework, relevant parameters such as flare/spot location and disc inclination can be extracted.

As mentioned, the orbiting spot model is not unique. Energy–shifted lines can be produced for example in outflows as well (see Turner, Kraemer & reeves 2004). However, the spot model makes definite predictions on the short timescale variability of the features. In this respect, it is much more appealing than other models because predictions can be tested and falsified. If the redshifted lines are really due to orbiting spots on the disc, they should vary on the orbital timescale at the spot location. If the flare/spot system lasts for more than one orbital period periodic modulations on both the emission line flux and energy should be seen, reflecting the orbital motion of the emitting spot and the different Doppler and beaming effects as the spot's orbit proceeds.

The Keplerian orbital timescale around a typical $10^7\ M_\odot$ black hole is about 10^4 s at 10 r_g. Therefore, some of the long and uninterrupted *XMM–Newton* observations (lasting about 10^5 s) potentially contains several cycles of orbital modulation. The orbiting spot model can then be tested by using long *XMM–Newton* observations of AGNs in which the redshifted features have been de-

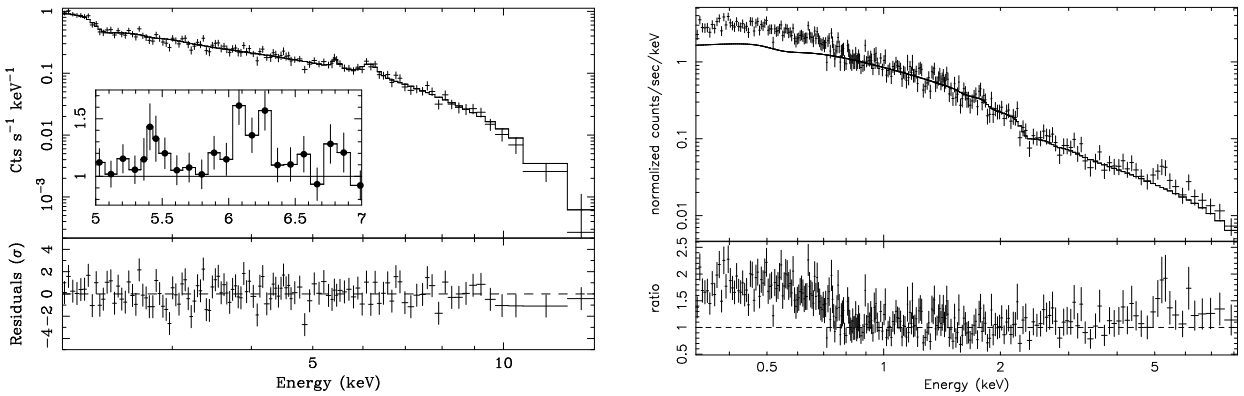

Figure 2. In the left panel we show the hard spectrum and data to model ratio from the first XMM–Newton observation of ESO 198–G24 where, besides emission around 6.4 keV, a feature is detected in emission around 5.7 keV (from Guainazzi 2003). In the right panel, we show a power law fit to the broadband XMM–Newton spectrum of ESO 113–G10. The emission line visible above 5 keV has a rest–frame energy of 5.4 keV and is detected at the 99 per cent level (from Porquet et al 2004). Long XMM–Newton follow–up observations are planned during AO4 to study the short timescale variability of the redshifted features in both sources.

tected.

3. THE CASE OF NGC 3516

We select one of the XMM-Newton observations of the bright Seyfert galaxy NGC3516 in which Bianchi et al (2004) reported the presence of an emission feature around 6.1 keV in addition to a stronger 6.4 keV Fe Kα line in the time-averaged spectrum. This is one of the most robust detection of a redshifted feature so far and the existence of a long *XMM–Newton* observation prompted us to study the short timescale variability in the Fe K band as a test for the orbiting spot model. Dovčiak et al (2004) have already studied the same dataset by splitting the observation in three time intervals about 27 ks long and they found that the feature is present in all intervals. However, if the orbiting spot model has to be tested, it is clear that a study at much shorter time–resolution is required.

There is another long *XMM–Newton* observation of NGC 3516 in which Turner et al (2002) reported the presence of a 6.2 keV emission feature which is however not present in the time–averaged spectrum but only towards the end of the observation indicating its transient nature. Since we want to study the variability of the feature on short timescales but for the longest possible period of time, we decided to study the first observation in which the feature seems to last for most of the exposure (Dovčiak et al 2004).

The time–averaged line profile of NGC 3516 during the selected observation is shown in Fig. 3. Two clear emission features are seen. The higher energy one is at 6.4 keV and is easily identified with a narrow Fe Kα emission line from a distant reflector such as the torus. The lower energy one is the feature we are interested in and is detected at 6.1 keV (hereafter the "red feature").

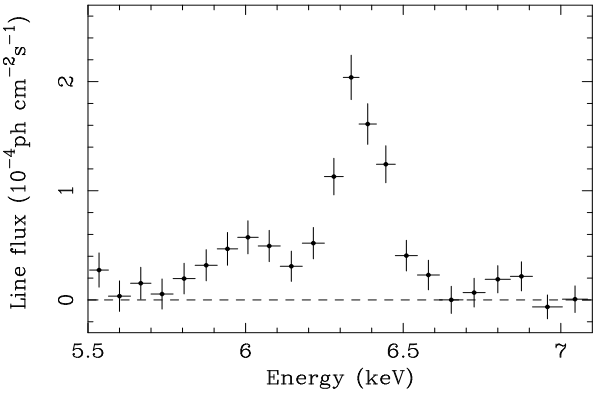

Figure 3. The time–averaged line profile of NGC 3516. Besides the Fe Kα line at 6.4 keV a redshifted emission feature is clearly seen around 6 keV (6.1 keV in the source rest–frame).

3.1. Variability analysis

The broad-band X-ray spectrum of NGC3516 is complex, as a result of modification by absorption and reflection components (Turner et al 2004). Since our interest is on the behaviour of the 6.1 keV feature only, we design our analysis method to avoid unnecessary complication: i) the energy band is restricted to 5.0–7.1 keV; ii) the continuum is determined by fitting an absorbed power-law to the data excluding the Fe line band (6.0–6.6 keV). In this way any spectral curvature induced by either a broad relativistic Fe line or absorption is modelled out and we are left with the narrow emission features only (the 6.4 keV Fe K line and the red feature).

To study the short timescale variability we first investigate time–resolved spectra at 5 ks resolution in time. Each individual 5 ks spectrum is fitted with the absorbed power law model and any excess emission above this con-

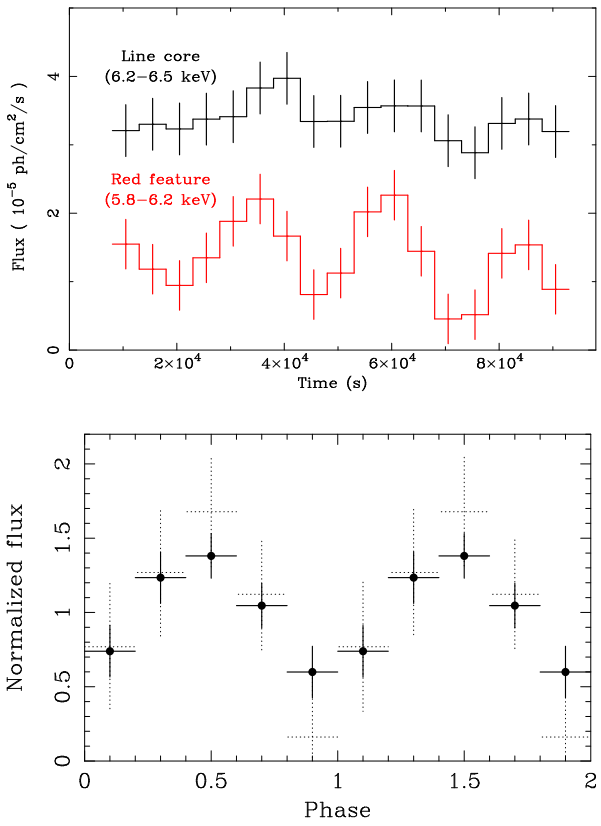

Figure 4. In the top panel we show two light curves extracted from the time–energy map of the excess emission. Each data point corresponds to a 5 ks time interval. Two energy bands are selected corresponding to the Fe Kα line core at 6.4 keV and to the red feature at 6.1 keV. The red feature light curve exhibits systematic variations suggesting a cyclic behaviour on a 25 ks timescale. In the bottom panel the red feature light curve is folded at 25 ks. The solid data refers to the folded light curved as extracted from the smoothed time–energy map of the excess emission, the dotted ones are from the original unsmoothed map. This shows that smoothing does not introduces spurious variability but only reduces the errors, as expected.

tinuum is recorded, corrected for the detector response, and used to construct a map of the excess emssion in the time–energy plane which is slightly smoothed to reduce intra–pixel noise (see Iwasawa, Miniutti & Fabian 2004 for details). The map suggests that systematic variation are taking place in the red feature energy band (5.8–6.2 keV in the observer frame).

In the top panel of Fig. 4 we show the light curves of the excess emission in two energy bands selected around the Fe K line core (6.2–6.5 keV band) and the red feature (5.8–6.2 keV) respectively. Errors are estimated via simulations as explained in Iwasawa, Miniutti & Fabian (2004). A simple χ^2 test reveals that the line core is well fitted by a constant while the same fit results in $\chi^2 = 36$ for 16 degrees of freedom for the red feature. The above results are confirmed through simulations. Moreover, as mentioned, the red feature appears to vary in a systematic way, the peaks and dips being always spaced by 25 ks. In the bottom panel of the same Figure, we show the result of folding the red feature light curve by using the evident 25 ks characteristic timescale. The light curve and the folding procedure suggest a cyclic behaviour with a 25 ks timescale. However, this result is based on four cycles only and it is difficult to secure any periodicity with such a small number of cycles. To investigate in more detail wheter noise can produce spurious cyclic variability we make use of Montecarlo simulations as detailed below.

3.2. Significance of the cyclic behaviour

Fitting the folded light curve with a constant provides an unacceptable fit of $\chi^2 = 24.5$ for 4 degrees of freedom. We do not consider this result as a clear indication for a periodicity, but we use it as a figure for Montecarlo simulations that are performed to assess the significance of the cyclic variability suggested by the data. We proceed as follows: in each simulation run, both the 6.4 keV line core and the red feature are assumed to remain constant at the flux observed in the time–averaged spectrum. The normalisation of the power law continuum is set to follow the 0.3–10 keV light curve. Each run consists of seventeen 5 ks spectra reproducing collectively the total exposure which is about 85 ks. From the simulated spectra, an image of the excess emission in the time–energy plane is obtained and smoothed, from which a light curve in the red feature energy band is extracted following exactly the same procedure as applied for the real data. The light curve is then folded at six trial periods between 15 ks and 40 ks with a 5 ks time–step (since the observation is about 85 ks long it does not make sense to consider longer trial periods) and the χ^2 value for a constant–fit is recorded and compared with that from the real data. The procedure is repeated 1000 times.

We find that only 0.2 per cent of the simulations show comparable or larger significance compared to the real data. Moreover, this is limited to the largest trial period of 40 ks (two cycles in the 85 ks long observation). None of the 1000 simulations show comparable periodic signals to the real data for the trial periods of 35 ks or shorter (i.e. we never observe spurious variability producing more than two cycles). The above test indicates it is unlikely for random noise to produce the cyclic patterns at the intervals of 25 ks as observed, providing a significance of 99.8 per cent for the cyclic behaviour. This result remains unchanged if the red feature light curve is characterized by red noise with the same power law slope and r.m.s. variability amplitude (2–3 per cent) as the continuum in NGC 3516. If the r.m.s. amplitude is artificially (and probably unreasonably) increased up to 35 per cent, the significance is reduced, but is still of about 98 per cent (see Iwasawa, Miniutti & Fabian 2004 for more details).

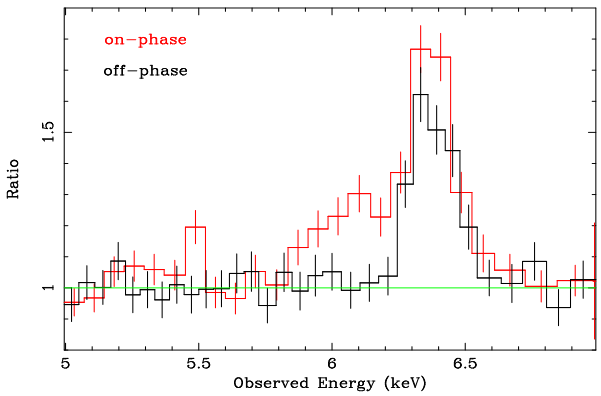

Figure 5. The two line profiles are obtained by performing phase–resolved spectroscopy following the light curve of the red feature. The red feature is detected only in the on–phase spectrum. It is absent in the off-phase spectrum the difference between the two being significant at the 4σ level.

3.3. Line profile variation in the on and off phases

Using the red feature light curve (top panel of Fig. 4) as a guide, we construct two spectra by selecting time–intervals in a periodic manner from the 'on' and 'off' phases to verify the implied variability in the red feature. The line profiles obtained from the two spectra are shown in Fig. 5. The two line profiles can be modelled with a double Gaussian model. The 6.4 keV core is found in both spectra with an equivalent width (EW) of 110 eV. While the 6.4 keV core remains similar between the two, there is a clear difference in the energy range of 5.7–6.2 keV due to the presence/absence of the red feature. In the on–phase spectrum, the red feature is centred at $6.13^{+0.10}_{-0.07}$ keV and has a flux of $2.1^{+1.3}_{-0.8} \times 10^{-5}$ ph cm^{-2} s^{-1} corresponding to an equivalent width of about 65 eV with respect to the continuum at the centroid energy. On the other hand, the red feature is not detected in the off–phase spectrum. If a line with the same centroid and width as in the on–phase spectrum is fitted to the off–phase data we only obtain a 90 per cent upper limit of $< 0.7 \times 10^{-5}$ ph cm^{-2} s^{-1} corresponding to an equivalent width < 20 eV. The variability detected between the two spectra is significant at 4σ confirming that the variability is real and present in the data.

3.4. Shorter timescales: flux and energy orbital modulation

The observed cyclic behaviour is exactly what is expected in the orbiting spot model: a periodic modulation should be seen corresponding to the orbital period of the spot and a cyclic behaviour is indeed observed. If this interpretation is correct the observed 25 ks characteristic timescale is the orbital period of the emitting spot. However, if the red feature is due to emission from an orbiting spot on the accretion disc, we do expect to see not only a periodic

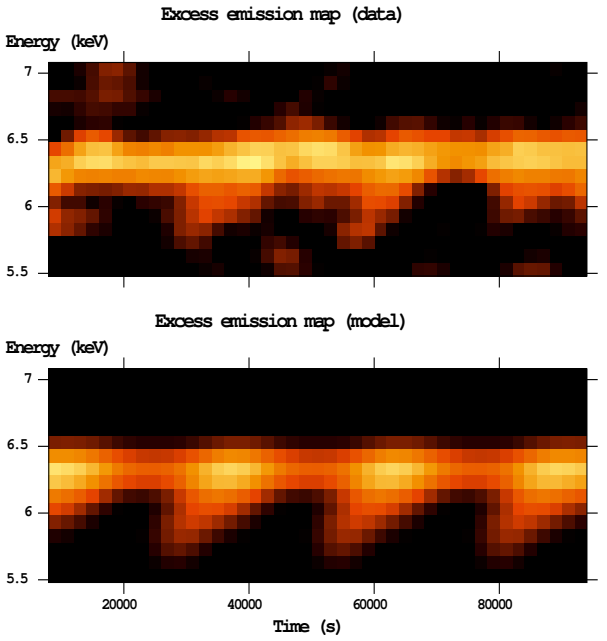

Figure 6. In the top panel we show the observed excess emission map at 2 ks resolution in time. In the bottom panel we show one of the theoretical maps constructed with the orbiting spot model. The brightest pixels correspond to about 15 counts of excess emission. The data–model agreement is surprisingly good and allows us to infer the parameters of the orbiting spot with good accuracy.

modulation in flux, but also in energy. This is because, as the spot orbits the black hole, it samples different regions of the accretion disc where different Doppler shifts are imprinted. As an example, when the spot is approaching to the observer, we expect a brighter and higher energy line, while when it is receading we should observe a fainter and lower energy line, due to the combined effect of relativistic Doppler and beaming effects. The image constructed from individual 5 ks spectra does not show any energy evolution. We therefore decided to investigate the feature evolution at a shorter timescale (2 ks).

The resulting (smoothed) image of the excess emission in the time–energy plane is shown in the top panel of Fig. 6 and exhibits further interesting behaviour. Beside the horizontal strip (representing the stable 6.4 keV Fe line) a saw–tooth pattern appears in the red feature energy band suggesting its energy evolution with time. The red feature emerges at about 5.7 keV and then increases its energy with time to merge with the 6.4 keV line. This behaviour appears to be repeated in each 'on' phase. If the characteristic variability timescale of 25 ks is interpreted as the orbital period of the emitting orbiting spot, this behaviour can be easily understood. Only the bright emission from the approaching side of the disc is seen and flux and energy both increase with time during the on phase. On the other hand, when the spot is on the receading side of the disc,the line emission is too faint to be detected (because of relativistic beaming away from

the observer) and we cannot see the opposite trend (flux and energy of the line decreasing with time during the off phase). However, this naive interpretation has to be tested with a model that takes into account all the relativistic effects on the emission from the spot on the disc.

To extract as much information as possible from the observed image, we adopt a simple model in which a flare is located above an accretion disc, corotating with it at a fixed radius. The flare illuminates an underlying region on the disc (or spot) which produces a reflection spectrum, including an Fe Kα line. The disc illumination is computed by integrating the photon geodesics in a Kerr spacetime from the flare to the disc, and is converted to local line emissivity. Then, the observed emission line profile is computed through the ray–tracing technique including all special and general relativistic effects (see Miniutti et al 2003; Miniutti & Fabian 2004). The main parameter of the model are the flare location, specified by its distance r from the black hole axis, its height above the accretion disc (h), and the accretion disc inclination i. We have computed the evolution of Fe K emission induced by an orbiting flare and simulated time-energy maps with the same resolution and smoothing as in the excess emission map of Fig. 6 (top panel) exploring the parameter space. A constant, narrow 6.4 keV core representing the Fe Kα line from distant material was also added to the model.

The bottom panel of Fig. 6 shows one of the theoretical time-energy maps we produced. This particular example assumes a flare with $(\,r\,,\,h\,) = (\,9\,,\,6\,)\;r_g$ and a disc inclination of 20°. By comparing the theoretical maps obtained with different spot's parameters with the data, we estimate that the flare must be located at a radius $r = (7 - 16)\;r_g$. The location of the flare (and of the irradiated spot on the disc) can be combined with the orbital timescale to provide an estimate of the black hole mass in NGC 3516. This is because the orbital period of the corotating flare/spot is related to its radial position by

$$T = 310\,[\,a + (\,r/r_g\,)^{3/2}\,]\,M_7 \quad [\,\mathrm{seconds}\,]\,, \qquad (1)$$

where M_7 is the black hole mass in units of $10^7\,M_{\odot}$ and a is the dimensionless black hole spin.

The most natural interpretation for the characteristic 25 ks timescale we observe is that it is the orbital period T of the emitting spot on the accretion disc. Therefore the only unknown in the above equation are the black hole spin and mass. Taking into account the uncertainty in a (which can take any value from 0 to 1), we estimate that the black hole in NGC 3516 has a mass of $M_{\rm BH} = (1 - 5) \times 10^7\;M_{\odot}$. This result is in very good agreement with reverberation mapping estimates ($1.7 \times 10^7\;M_{\odot}$ Onken et al 2003; 2.3×10^7 Ho 1999) providing further support for our interpretation.

Our results indicate that present X-ray missions such as *XMM–Newton* are already probing the spacetime geometry in the vicinity of supermassive black holes if their observational capabilities are pushed to the limit. Future observatories such as *XEUS* and *Constellation-X*, which are planned to have much larger collecting area at 6 keV, will be able to exploit this potential and map the strong field regime of general relativity with great accuracy.

ACKNOWLEDGMENTS

We thank the European Space Astronomy Centre (ESAC) and the Organizing Committee for organizing such a beautiful conference in El Escorial. The work presented here is based on observations obtained with *XMM-Newton*, an ESA science mission with instruments and contributions directly funded by ESA Member States and NASA. GM and KI thank the PPARC for support. ACF thanks the Royal Society for support.

REFERENCES

[1] Bianchi S. et al, 2004, A&A, 422, 65

[2] della Ceca R. et al, 2005, ApJ, 627, 706

[3] Dovčiak M. et al, 2004, MNRAS, 350, 745

[4] Fabian A.C. et al, 2002, MNRAS, 335, L1

[5] Guainazzi M., 2003, A&A, 401, 903

[6] Ho L.C., 1999, in Observational Evidence for BHs in the Universe, ed. S.K. Chakrabarti (Dordrecht: Kluwer), 157

[7] Homan J. et al, 2003, ApJ, 586, 1262

[8] Iwasawa K. et al 1999, MNRAS, 306, L19

[9] Iwasawa K., Miniutti G., Fabian A.C., 2004, 355, 1073

[10] Miller J.M. et al, 2002, ApJ, 570, L69

[11] Miniutti G. et al, 2003, MNRAS, 344, L22

[12] Miniutti G., Fabian A.C., 2004, 2004, MNRAS, 349, 1435

[13] Miniutti G., Fabian A.C., Miller J.M., 2004, 351, 466

[14] Onken C.A. et al, 2003, ApJ, 585, 121

[15] Pecháček T. et al, 2005, A&A, 441, 855

[16] Porquet D. et al, 2004, A&A, 427, 101

[17] Rossi S. et al, 2005, MNRAS, 360, 763

[18] Tanaka Y. et al, 1995, Nature, 375, 659

[19] Turner T.J. et al, 2002, ApJ, 574, L123

[20] Turner T.J., Kraemer S.B., Reeves J.N., 2004, ApJ, 603, 62

[21] Turner T.J. et al, 2004, ApJ, 618, 155

[22] Wilms et al, 2001, MNRAS, 328, L27

[23] Yaqoob T. et al, 2003, ApJ, 596, 85